Contrib. Mineral. Petrol. 64, 273–302 (1977)

Contributions to Mineralogy and Petrology

Structural Characterization of Labradorite-Bytownite Plagioclase from Volcanic, Plutonic and Metamorphic Environments

Timothy L. Grove*

Hoffman Laboratory, Harvard University, 20 Oxford Street, Cambridge, Massachusetts 02138, USA

Abstract. The transmission electron microscope and the electron microprobe are used to characterize calcic plagioclase (An_{65} to An_{85}) from a variety of geological environments. The cooling histories of samples from volcanic, plutonic and metamorphic environments are estimated and the transformation and exsolution sequence is inferred from observations in the transmission electron microscope. Several distinctive textural modifications occur depending both on bulk composition and cooling history. (1) Exsolution occurs in increasingly calcic bulk compositions upon slower cooling, and the coexisting phases are An_{66} intermediate plagioclase and An_{85-90} $P\bar{1}$, $c=14$ Å plagioclase in the sample from the metamorphic environment, (2) the morphology of b antiphase boundaries (APBs) in An_{75} to An_{85} plagioclase changes from smoothly curving (rapid cooling and calcic compositions) to zig-zag (slower cooling or sodic compositions). (3) The concentration of defects in the intermediate plagioclase superstructure changes from a high density in rapidly cooled plagioclase to a lower density in slowly cooled plagioclase. In all plagioclases except for the rapidly cooled, volcanic specimens there is evidence in images and diffraction patterns for short-range ordered domains with $P\bar{1}$ symmetry. The observations allow the microstructure of a single zoned plagioclase to be used as an indication of the geologic environment under which it cooled.

1.1. Introduction

Although the relations between structural forms of plagioclase seem impossibly complex, a characterization of phase transformations and exsolution relations can provide a potentially sensitive indication of geologic history. Huttenlocher (1942) and Jäger and Huttenlocher (1955) first observed exsolution lamellae

* *Present address:* Department of Earth and Space Sciences, State University of New York, Stony Brook, New York 11794, USA

in bytownite and Nissen (1968) identified the two plagioclases as having the anorthite and the intermediate plagioclase structures. Recent transmission electron microscopic (TEM) studies (Heuer et al., 1972; Müller et al., 1972; Nord et al., 1974; McLaren, 1974; McConnell, 1974; Nissen, 1974) have revealed exsolution textures in igneous plagioclases (An_{74-85}) that are below the resolution of optical microscopy and have shown antiphase domains that record structural transformations. Thus, bytownitic plagioclase undergoes exsolution as well as structural transformations, and plagioclases that grow under different geologic conditions may show distinctive exsolution textures and antiphase domain morphologies.

The transmission electron microscope (TEM) is used in this study to analyze and interpret submicroscopic structures in plagioclase of An_{65} to An_{85} bulk composition. Selected-area electron diffraction patterns and antiphase domains are used to determine the structural type of the plagioclase and to infer the transformation sequence. Exsolution textures are characterized both as a function of cooling history and bulk plagioclase composition. Observations are made on specimens that formed under a variety of geologic environments and are incorporated into a cooling history vs. composition characterization for labradorite-bytownite plagioclase.

1.2. Method of Study

Specimens of plagioclase were selected from volcanic, shallow-plutonic, deep-seated plutonic and metamorphic environments. These four geologic settings more or less span the cooling histories experienced by terrestrial rocks and allow observation of the range of submicroscopic textures expected to form in nature. For each sample the cooling history was crudely estimated using the method of Lovering (1935). Plagioclase grains were analyzed with the electron microprobe before they were observed with the transmission electron microscope. Heuer and Nord (1976a) and Nord et al. (1973) emphasize that antiphase domain morphology and size change in response to bulk chemistry as well as cooling history. Therefore, before the sample can be assigned a cooling history, the bulk composition of the plagioclase must be determined. This problem has plagued plagioclase crystallography for years, but it is easily overcome combining the electron microprobe with transmission electron microscopy.

Inference of Structural History

Before proceeding with a description of the submicroscopic textures, a consideration of the assumptions involved in deducing the transformation-exsolution history of plagioclase is necessary. Much discussion has taken place in the literature concerning the interpretation of antiphase boundaries in anorthite (Müller et al., 1973; Heuer et al., 1972; Wenk et al., 1973). The assumptions and observations are lucidly discussed by Heuer and Nord (1976a) and their conclusions are adopted in this study. The high-temperature structure that is

the precursor to the periodic antiphase structure of intermediate plagioclase has also been the subject of some discussion (McConnell, 1974; McLaren and Marshall, 1974; Wenk et al., 1975) and some possibilities for the transition sequence are discussed in the observation section.

Structural Transformations in Anorthite

The recent application of transmission electron microscopy (TEM) to the study of structural variations in anorthite has elucidated the sequence of phase transformations proposed from earlier X-ray crystallographic studies (Laves and Goldsmith, 1951; Gay, 1953). The existence of three structural forms; a high-temperature form with a random distribution of tetrahedrally coordinated Al and Si ($C\bar{1}$, $c=7$ Å), an ordered body-centered form ($I\bar{1}$, $c=14$ Å), and a low-temperature primitive form ($P\bar{1}$, $c=14$ Å), has been inferred from observation of antiphase domains and the transformation sequence from high to low temperature is

$$C\bar{1} \rightarrow I\bar{1} \rightarrow P\bar{1}.$$

Class *a* ($h+k=2n$, $l=2n$) reflections are related to the $C\bar{1}$, $c=7$ Å structure, class *b* ($h+k=2n+1$, $l=2n+1$) reflections result from the transformation to $I\bar{1}$, $c=14$ Å symmetry and class *c* ($h+k=2n$, $l=2n+1$) and *d* ($h+k=2n+1$, $l=2n$) reflections arise from the transformation to $P\bar{1}$ symmetry. Two types of antiphase domains are possible, those related to the $C\bar{1}$ to $I\bar{1}$ transition (*b* ABPs) visible in TEM images taken with *b* reflections operating and antiphase boundaries observed with the class *c* and *d* reflections (*c* APBs) that form during the $I\bar{1}$ to $P\bar{1}$ transition. In an $I\bar{1}$ structure the possible fault vectors $R=1/2[110]$ and $R=1/2[001]$ are indistinguishable and both describe the displacement across the APB equally well. In this study the existence of the $C\bar{1}$ to $I\bar{1}$ transition is inferred from the observation of antiphase boundaries visible with *b* reflections. In the $P\bar{1}$ structure $R=1/2[111]$ is the displacement vector for APBs related to the $I\bar{1}$ to $P\bar{1}$ transition, and $R=1/2[110]$ and $R=1/2[001]$ become distinguishable. Evidence for $R=1/2[110]$ has been presented by Müller et al. (1973) and McLaren and Marshall (1974). A dark field micrograph taken with a *c* reflection (Fig. 4c of Nord et al., 1973) shows *b* APBs related to the $C\bar{1}$ to $I\bar{1}$ transformation and *c* APBs related to the $I\bar{1}$ to $P\bar{1}$ transformations. Hence, both $R=1/2[001]$ and $R=1/2[110]$ are possible fault vectors. Although there still seems to be some discussion as to the precise nature of fault vectors in $P\bar{1}$ anorthite, the presence of two distinct domain morphologies (Heuer and Nord, 1976a), one imaged with *b* reflections and one observed with *c* reflections proves the existence of the $C\bar{1}$ to $I\bar{1}$ and the $I\bar{1}$ to $P\bar{1}$ transition.

Contrast from Intermediate Plagioclase

Intermediate plagioclase occurs over the compositional range An_{25} to An_{75} and is characterized by the presence of class *a* reflections, class *e* reflections occuring as pairs of satellites around the positions of class *b* reflections and

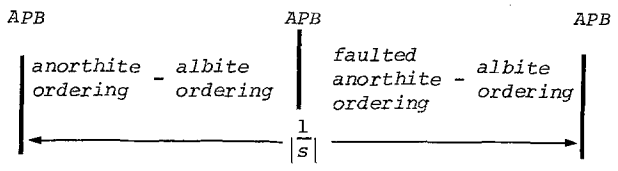

Fig. 1. Schematic model of the periodic antiphase structure of intermediate plagioclase. An antiphase boundary is encountered twice during each repeat unit

f satellites that are sometimes present in pairs about *a* reflections. Both X-ray structural analyses (Toman and Frueh, 1975a, b) and TEM studies (McConnell and Fleet, 1963) have shown that the superstructure of intermediate plagioclase is a periodic antiphase structure. In addition, each periodic antiphase domain consists of one region that is Na-rich (albite-like) and another region that is Ca-rich (anorthite-like) (Fig. 1). The existence of *e* satellites around the position of *b* reflections indicates that the fault vector for periodic antiphasing is $R=1/2[110]$ or $1/2[001]$. Although the superstructure was originally described using the reciprocal lattice vector s (Bown and Gay, 1958) measured from the position of the *b* maxima to an *e* satellite, the size of one periodic antiphase domain is half the complete periodicity or 2s. Since the distance between a pair of *e* satellites or an *a–f* reflection pair corresponds to 2s, an image of the superlattice fringes can be observed which has a periodicity corresponding to the spacing of the antiphase boundaries $1/(2|s|)$.

The superlattice finge images obey the rules of lattice fringe images as discussed by Hirsch et al. (1965), and any interpretation of change in fringe periodicity and orientation must be made with caution since small deviations from the Bragg condition and changes in foil thickness will affect the lattice fringe image.

1.3. Cooling History of the Plagioclases

The plagioclase specimens chosen from volcanic (Mariana Islands) epizonal plutonic (Ardnamurchan, Scotland), catazonal plutonic (Nain, Labrador) and high-grade regional metamorphic (Warwick, Massachusetts) environments are discussed in the Appendix. A time-temperature cooling history for the igneous rocks was estimated by solving the heat equation after Lovering (1935). The assumptions and oversights in Lovering's treatment obviously simplify an extremely complex natural process and the results of the calculations presented here are only of order-of-magnitude accuracy at *best*. However, the calculations allow a comparison to be made between the three igneous rocks (Fig. 2). The Warwick calc-silicate cooling history was estimated using erosional and uplift rates, maximum temperature of metamorphism, and a geothermal gradient. Using the cooling rate calculations to establish time-temperature paths for the three igneous rocks and for the Warwick metasediment, the total time-integrated cooling rates calculated are: (1) 6×10^{1} °C/yr for the Marina andesite;

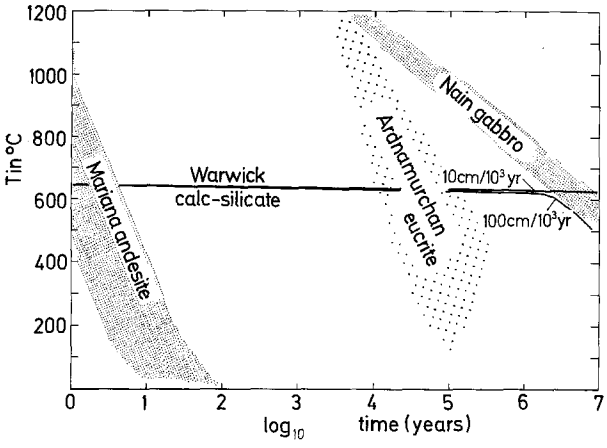

Fig. 2. Cooling histories plotted as a function of temperature and $\log_{10}$ time. See Appendix for details of calculation

(2) 5×10^{-3} °C/yr for the Ardnamurchan eucrite; (3) 9×10^{-5} °C/yr for the Nain gabbro; (4) 5×10^{-6} °C/yr for the Warwick calc-silicate.

Considering the large errors in the calculations, the differences in the time integrated cooling rate between the Nain gabbro and the Warwick calc-silicate are not significant. However, the initial temperature experienced by the Nain gabbro is that of a plutonic environment while that experienced by the Warick calc-silicate was characteristic of regional metamorphism.

2.1. Experimental: Mariana Andesite and Ardnamurchan Eucrite

Thin sections were prepared with a single polished surface and specimens of appropriate crystallographic orientation were selected with the optical microscope. The plagioclase specimens were mounted between standard three millimeter copper washers and analyzed with the electron microprobe. Since the Ardnamurchan and Mariana plagioclases are chemically zoned, electron microprobe analysis is the only reliable method for estimating the composition of the region to be observed with the TEM. The analyzed specimens were thinned by ion bombardment.

2.2. Warwick Calc-Silicate and Nain Gabbro

Specimens of appropriate orientation and chemical composition were chosen from standard thin sections. An estimate of chemical composition was made by comparing the textures observed in the TEM specimen with those observed in thin section and analyzed with the electron microprobe. It was possible to distinguish between labradorite regions, two-phase intergrowths and bytownite regions in Warwick specimens, and little compositional variation was found within each of the three textural types (see Appendix). Compositions for the Nain TEM specimens were also estimated by textural comparison with material previously analyzed using the electron microprobe.

2.3. Operating Conditions

The plagioclase specimens were examined with JEM7 and Philips EM300 microscopes operating at 100 kV. Most observations were made in dark field because many of the g's of interest had

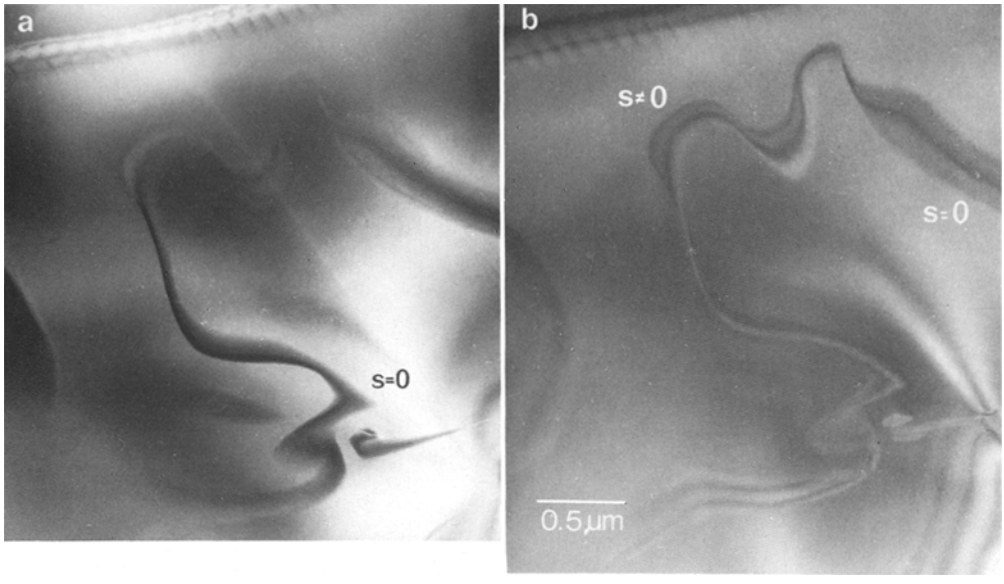

Fig. 3a and b. *Mariana plagioclase, An_{79}.* **a** Curving *b* antiphase boundaries. DF, $g=1\bar{2}1$. **b** Same region as (**a**). APBs show contrast characteristic of π faults. DF, $g=3\bar{2}\bar{1}$

small structure factors and commonly many beams were contributing to diffraction. Electron diffraction patterns were analyzed as an aid in determining *g* for dark field images using program DSPAC (Booth et al., 1973).

3.1. TEM Observation of Mariana Plagioclase (An_{76} to An_{80})

Dark field images using *b* reflections (Fig. 3) reveal smoothly curving antiphase boundaries (APBs) that are interpreted as thermal APBs (Marcinkowski, 1963) that formed during the transformation from $C\bar{1}$ to $I\bar{1}$. Contrast observed on the Mariana plagioclase *b* APBs is consistent with that of $\alpha=\pm\pi$ faults (van Landuyt et al., 1964). Since extinction distances (ξ_g) for *b* reflections are large, only 1 or 2 fringes are visible on the APB. Regions in which $s=0$ (Fig. 3a) have a central dark fringe symmetrically surrounded by light fringes. In regions where $s\neq 0$ the symmetry of the fringe is destroyed (Fig. 3b), and fringes are dark on one end, bright on the other end, and the center of the fringe is at the boundary between a dark and light fringe. Similar observations have been made by McLaren and Marshall (1974) for $s=0$. Weak contrast is visible when *b* APBs are viewed with *a* reflections in a manner similar to that reported by Wenk et al. (1973) in lunar plagioclase. The contrast is assumed to result from many beam interactions that are unavoidable from the small reciprocal cell of plagioclase. Occasionally weak, diffuse class *c* reflections are visible in electron diffraction patterns along with the sharp *a* and *b* reflections. The *c* reflections are streaked along [0k0]* repiprocal lattice rows in the [100] zone, and form a continuous band of diffuse intensity.

3.2. TEM Observations of Ardnamurchan Plagioclase

The TEM observation of the Ardnamurchan plagioclase reveal 3 textural types that are found in the compositional ranges An_{68} to An_{74}, An_{75} to An_{78} and An_{80} to An_{81}. Plagioclase between An_{68} and An_{74} is distinguished by the presence of a two-phase intergrowth and the absence of *b* APBs. From An_{75} to An_{78} two-phase intergrowths and *b* APBs are observed and plagioclase more calcic than An_{80} is distinguished by the presence of *b* APBs and the absence of exsolved intermediate plagioclase.

An_{68} to An_{74}

Electron diffraction patterns indicate the presence of two plagioclases, an intermediate plagioclase and an $I\bar{1}$ plagioclase (Fig. 4). Strong *a* reflections are surrounded by weak *f* satellites and *b* reflections that are barely visible in An_{68} but sharp in An_{73-74} (Fig. 4a) are surrounded by class *e* satellites. Diffuse curved streaks are present between *e* satellites and the *b* reflection, and overexposed electron diffraction patterns show diffuse bands of intensity parallel to the [0k0]* and [00l]* lattice rows on the [100] pole (Fig. 4b). This diffuse intensity is at a maximum in the position of class *c* reflections.

A lamellar modulation similar to that observed by McLaren (1974) which he called quasi-periodic lamellar structure is present in dark field micrographs taken with *a* reflections. The 2 directions of lamellae appear to be approximately parallel to (010) and (001) in [100] zone orientations (Fig. 4d), (010) and (100) in the [001] zone orientation (Fig. 4c), and (010) in the [101] zone. The texture is present over the entire compositional range of observation (An_{68} to An_{81}) and does not appear to be related to the intergrowths of $I\bar{1}$ and intermediate plagioclase. McLaren reasoned that lamellar modulation contrast could result from a slight misorientation between adjacent lamellae, but could find no evidence in diffraction patterns of his An_{75} sample that explained the effect. The diffuse streaks present in the position of *c* reflections (Fig. 4b) may explain the nature of the lamellar structure, since the streaks are approximately perpendicular to the dark-light lamellar contrast observed in Figure 4d (the micrograph and diffraction pattern are of the same area). Thus, the lamellar modulation may indicate the presence of short-range ordered domains that are $P\bar{1}$-like in nature.

Dark field images from *e* and *b* reflections show a texture that has a different orientation than the lamellar modulation and is related to intergrowths of intermediate plagioclase and $I\bar{1}$ plagioclase (Fig. 5). Images taken in the same area but using an *e* satellite and *b* reflection, respectively, to form the image show the difference in contrast from intermediate and $I\bar{1}$ plagioclase. The intermediate plagioclase (Fig. 5a) gives the appearance of a wormy intergrowth of domains. However, the contrast from *b* reflections shows that the domains are separated by $I\bar{1}$ plagioclase lamellae that are 50 to 100 Å thick and range in orientation from parallel to $(03\bar{1})$ to $(01\bar{1})$. The wormy texture is again shown in An_{68} (Fig. 5c) in an orientation close to the [101] zone and in Figure 5d when the

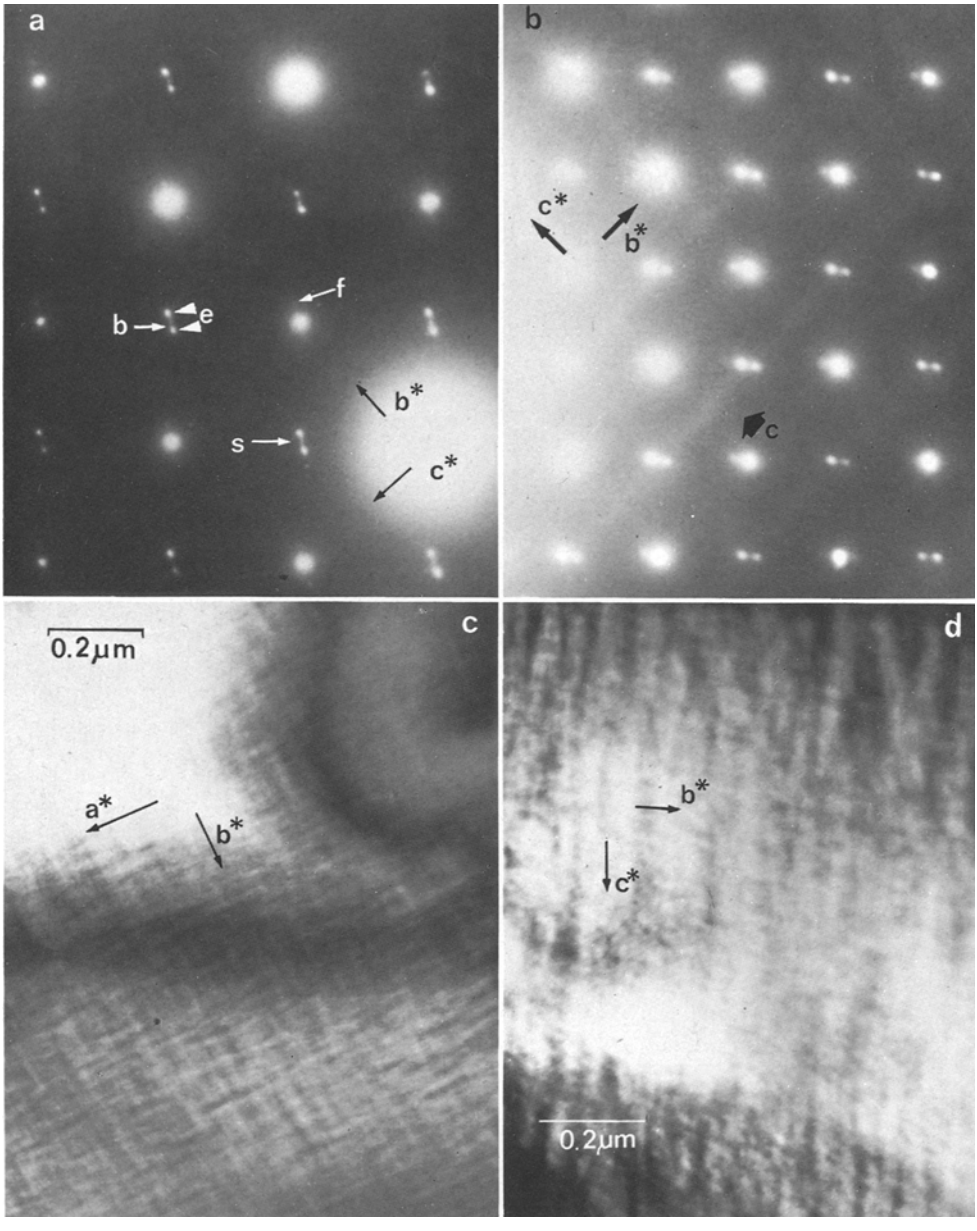

Fig. 4a–d. *Ardnamurchan plagioclase.* **a** Electron diffraction pattern of An_{73-74} shows *a*, *e* and *f* reflections of intermediate plagioclase and *b* reflections of $I\bar{1}$ plagioclase. Curved streaks are present between *e* pairs and *b* reflections at s. [100] zone axis. **b** Over-exposed diffraction pattern taken in the same region as **d**. Weak diffuse intensity parallels [0k0]* and [00l]* lattice rows with maximum intensity at the position of *c* reflections. **c** Electron micrograph of lamellar modulation in An_{68} observed near [001] zone axis. Trace of modulation is approximately parallel to b^* and a^*. DF, $g=1\bar{3}0$. **d** Lamellar modulation observed in [100] orientations is perpendicular to the direction of streaked intensity. DF, $g=04\bar{2}$ [image taken in region of diffraction pattern (**b**)]

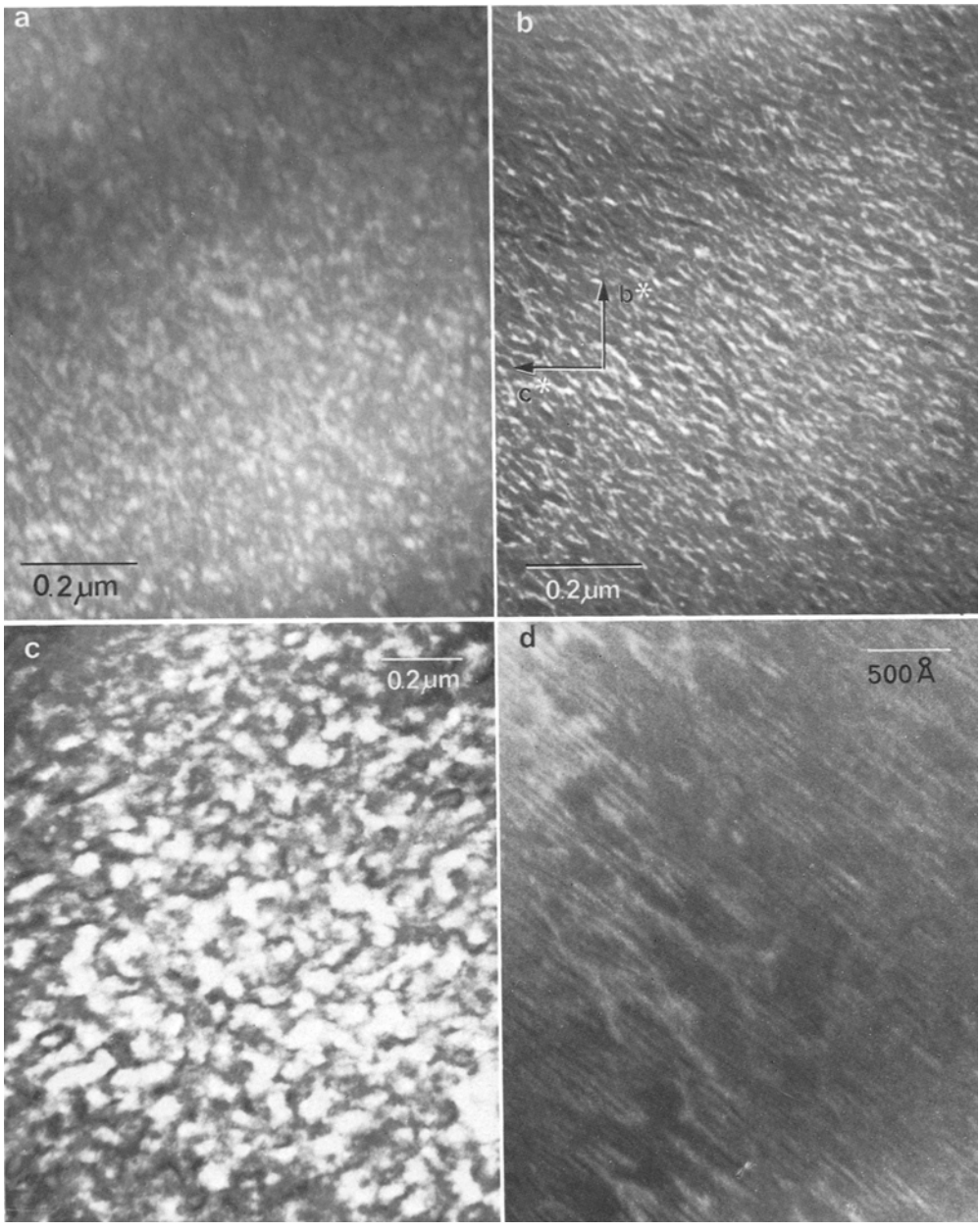

Fig. 5a–d. *Ardnamurchan plagioclase.* **a** Electron micrograph in An_{70-71} shows wormy intergrowth of intermediate plagioclase domains. DF, $g=013$, $s=0$ for one *e* satellite. **b** Same region as (**a**). $I\bar{1}$ plagioclase portion of two-phase intergrowth in An_{70-71}. $I\bar{1}$ lamellae have components parallel to trace of $(03\bar{1})$ and $(01\bar{1})$ planes. DF, $g=013$, $s=0$ for *b* reflection. **c** Electron micrograph of An_{68}. Intermediate plagioclase domains viewed near [101] zone axis. DF, $g=1\bar{4}\bar{1}$, $s=0$ for one *e* reflection. **d** Electron micrograph of intermediate plagioclase domains in An_{73-74}. Superstructure is continuous over small areas. DF, $g=0\bar{3}1$, $s=0$ for an *e* satellite pair

Bragg condition is satisfied for both members of the *e* satellite pair. Note that sometimes the periodic antiphase boundaries of the intermediate plagioclase appear to continue into an adjacent domain, but that sometimes the periodic antiphase domains appear to be offset at the boundary. This texture is similar to that observed in igneous and metamorphic intermediate plagioclase (McLaren and Marshall, 1974; Wenk et al., 1975; Hashimoto et al., 1976) where it has not been associated with a two phase intergrowth. In Ardnamurchan it is associated with the beginnings of exsolution of an $I\bar{1}$ and an intermediate plagioclase in which the intermediate plagioclase predominates over the $I\bar{1}$ phase. The $I\bar{1}$ lamellae are small enough that the two phases overlap, resulting in a complex image that consists of predominantly intermediate plagioclase with tiny stringers of $I\bar{1}$ plagioclase distributed throughout.

An_{75} to An_{78}

The diffraction geometry of An_{75} to An_{78} Ardnamurchan plagioclase (Fig. 6a) is quite different from that observed in An_{68} to An_{74}. Sharp *a* and *b* reflections possess curved streaks with length and orientation equal to s for intermediate plagioclases in the compositional range An_{65} to An_{73}, and similar to the streaks observed by Nord et al. (1974) in bytownites (An_{80-82}) from the Stillwater igneous complex. The streaks suggest a series of short-range ordered regions in the Ardnamurchan plagioclase with intermediate plagioclase-like structures, and indicate that the periodic structure varies in size and orientation and is not continuous or large enough to diffract as a coherent superstructure phase. Weak, diffuse *c* reflections are also present.

A two-phase intergrowth consisting of an $I\bar{1}$ phase and an intermediate plagioclase phase is observed with the TEM (Fig. 6a). The $I\bar{1}$ phase predominates in the An_{75} to An_{78} compositions, and the orientation of exsolved intermediate plagioclase is similar to that observed for the $I\bar{1}$ lamellae in An_{68} to An_{74}. Zig-zag antiphase boundaries in the $I\bar{1}$ phase are observed in dark field using *b* reflections, and the APB morphology and exsolution texture are similar to that observed in Stillwater plagioclase. The presence of *b* APBs indicates that a $C\bar{1}$ to $I\bar{1}$ transition took place followed by the formation of the two-plagioclase intergrowth.

An_{80} to An_{81}

Diffraction patterns of An_{80} to An_{81} plagioclase contain sharp *a* and *b* reflections and very weak *c* reflections. Large curving antiphase boundaries are visible with *b* reflections (Fig. 7), and a zig-zag texture has developed on the boundaries but not to the extent observed in An_{75-78} plagioclase, or in the Stillwater plagioclase. No evidence for a two-plagioclase intergrowth is found in either the electron diffraction patterns or the electron micrographs. A lamellar modulation similar in morphology to that observed in An_{68-74} and An_{75-78} is found in An_{80-81} Ardnamurchan plagioclase, and is visible in dark field micrographs

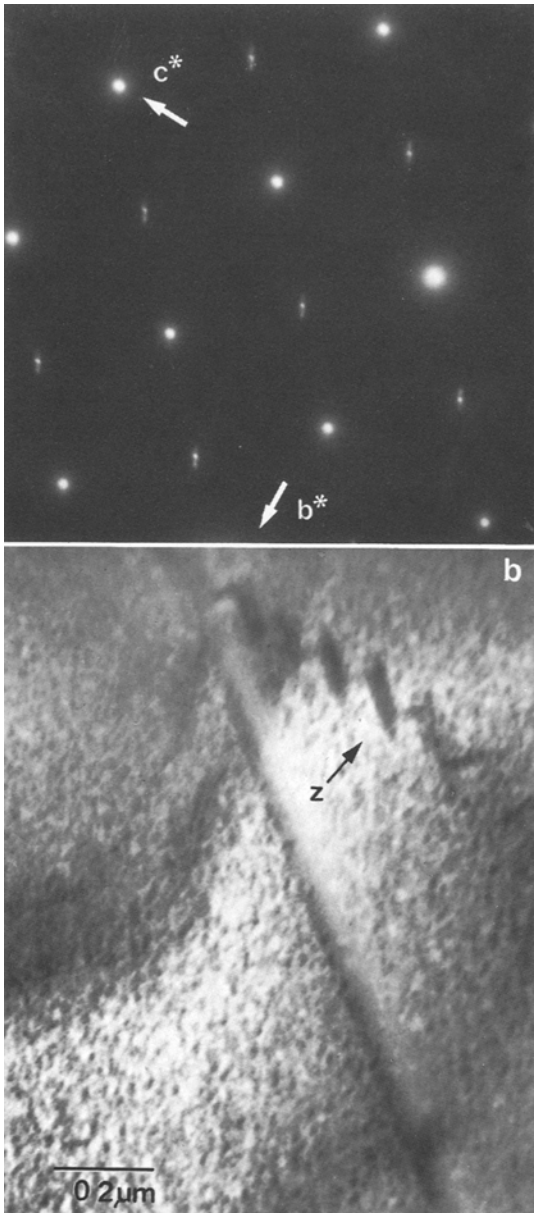

Fig. 6a and b. *Ardnamurchan plagioclase*
a Electron diffraction pattern of An_{78} shows *b* reflections with diffuse streaks. Streak orientation approaches that of s for calcic intermediate plagioclase (An_{65}-An_{73}). Present in diffraction pattern, but not visible on photo are weak type *c* reflections. [100] zone axis
b Electron micrograph of An_{78} shows zig-zag antiphase boundary at z and two-plagioclase intergrowth. DF, $g=013$, $s=0$ for *b* reflection

taken with *a* reflections. Contrast on *b* APBs is visible with class *a* reflections, and is weak for some *g*'s but stronger for others. Although the visibility of *b* APBs with *a* reflections may result from dynamic interactions, not all the effects observed in Ardnamurchan plagioclase can be accounted for using this explanation. It is possible that the antiphase boundaries have served as nuclea-

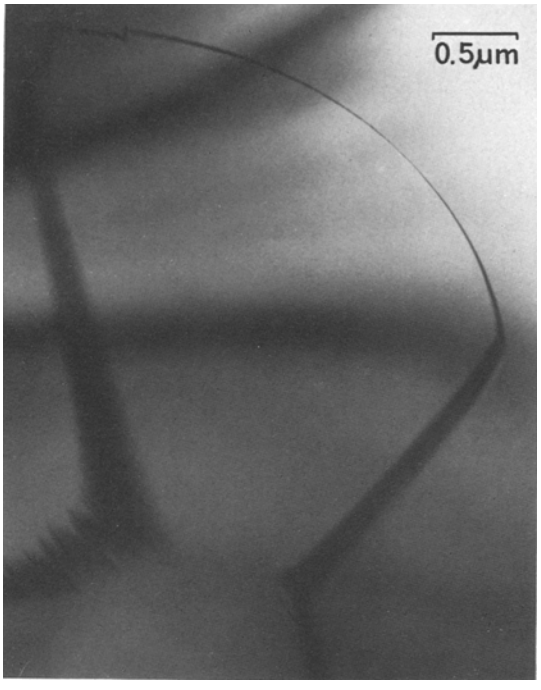

Fig. 7. *Ardnamurchan plagioclase.* Electron micrograph of *b* antiphase boundary in An_{81}. APB has begun to develop a zig-zag texture. DF, $g=0\bar{1}1$

tion sites for two phase intergrowths or that some other structural defect has formed on the APB.

3.3. TEM Observations of Nain Plagioclase, An_{66-70}

Optically visible two-plagioclase intergrowths found in Nain plagioclase of bulk composition An_{66} to An_{70} have textures and diffraction geometries similar to those observed by Grove (1976) and Nissen (1974) in metamorphic bytownites. Two directions of exsolution are present with orientations of $(03\bar{1})$ and $(30\bar{1})$ (Fig. 8a). Within the intermediate plagioclase (Fig. 8a) is a lamellar modulation texture, and single crystal X-ray photos of optically homogenous Nain plagioclase (An_{66}) contain weak *c* reflections, suggesting the presence of $P\bar{1}$-like domains. Estimates of the volume proportion of the calcic phase made from electron micrographs range from 5 to 20%. If the end-members of the Nain plagioclase intergrowth are assumed to be An_{66} and An_{85} (Cliff et al., 1976), the volume fraction of lamellae should approach 20% for an An_{70} bulk composition, consistent with the estimates made from electron micrographs.

δh, δk and δl were determined for the intermediate plagioclase host of the two-phase intergrowth (Table 1). The orientation of s is similar to that determined for An_{64-67} (Gay, 1956), but the magnitude of s is less than expected.

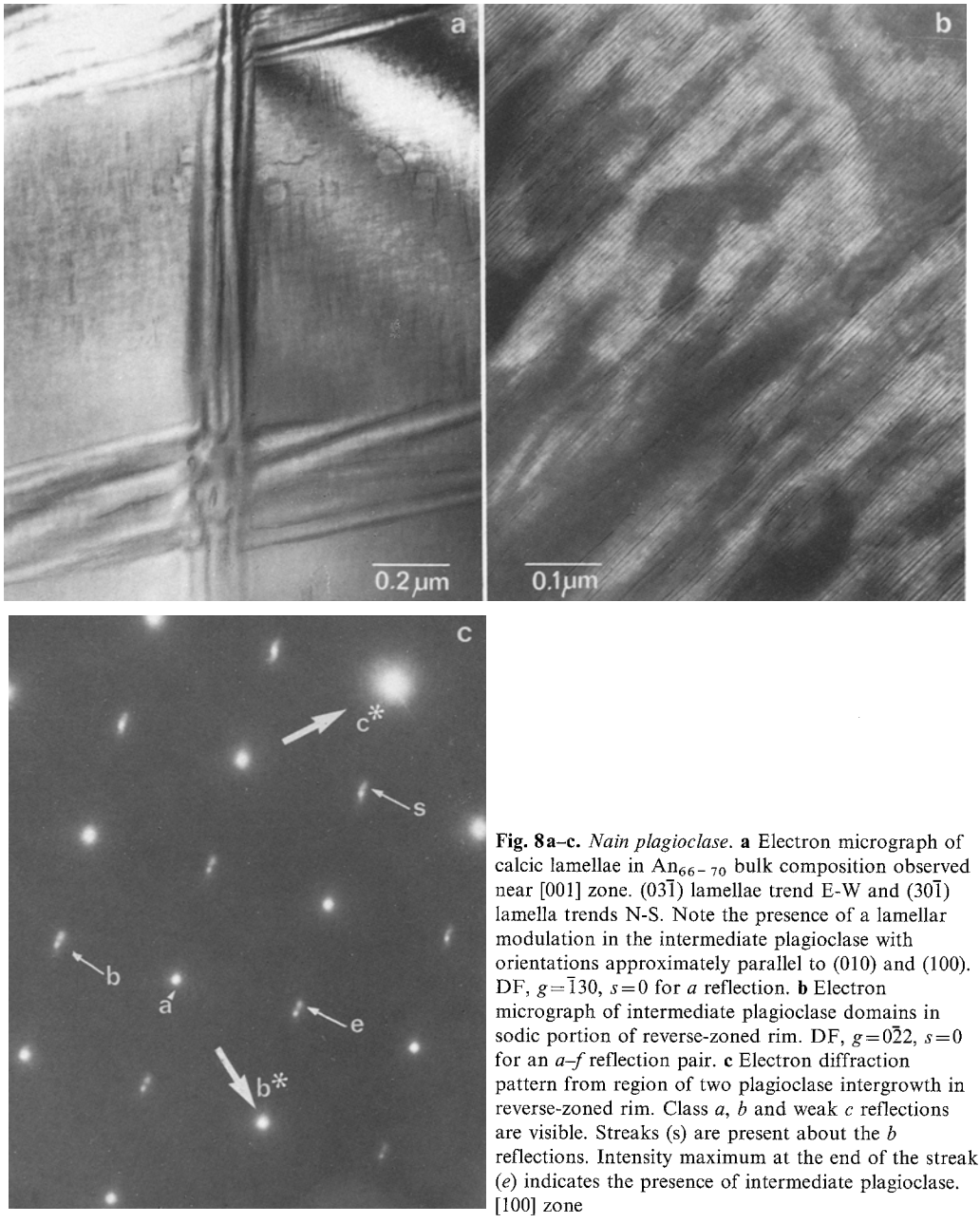

Fig. 8a–c. *Nain plagioclase.* **a** Electron micrograph of calcic lamellae in An_{66-70} bulk composition observed near [001] zone. $(03\bar{1})$ lamellae trend E-W and $(30\bar{1})$ lamella trends N-S. Note the presence of a lamellar modulation in the intermediate plagioclase with orientations approximately parallel to (010) and (100). DF, $g=\bar{1}30$, $s=0$ for *a* reflection. **b** Electron micrograph of intermediate plagioclase domains in sodic portion of reverse-zoned rim. DF, $g=0\bar{2}2$, $s=0$ for an *a–f* reflection pair. **c** Electron diffraction pattern from region of two plagioclase intergrowth in reverse-zoned rim. Class *a*, *b* and weak *c* reflections are visible. Streaks (s) are present about the *b* reflections. Intensity maximum at the end of the streak (*e*) indicates the presence of intermediate plagioclase. [100] zone

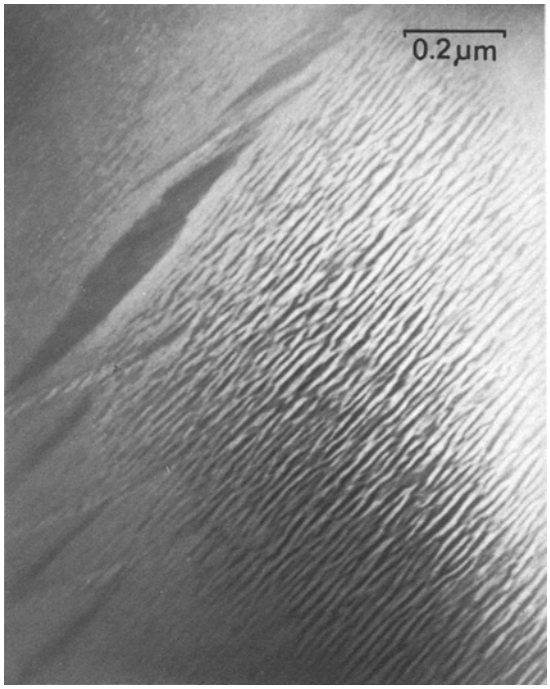

Fig. 9. *Nain plagioclase.* Electron micrograph from calcic region of reverse-zoned rim shows zig-zag antiphase boundaries and the two-phase intergrowth of $I\bar{1}$ and intermediate plagioclase. DF, $g=03\bar{1}$, $s=0$ for *b* reflection

TEM Observations in Nain Plagioclase, An_{72} to An_{85}

An optically homogeneous reverse-zoned rim of plagioclase surrounds the two-phase intergrowths (see Appendix) and varies in composition from An_{72} to An_{85}. Two textural types are distinguishable in the reverse-zoned rim. One is found in the sodic portion of the rim and the other is in the calcic portion. Electron diffraction patterns taken in the sodic portion indicate that both intermediate plagioclase and minor amounts of a calcic $I\bar{1}$ phase are present. Superlattice fringe images of the intermediate plagioclase phase (Fig. 8b) show the wormy texture observed in Ardnamurchan.

Electron diffraction patterns taken in the calcic region of the rim contain sharp *a* and *b* reflections surrounded by curved streaks (Fig. 8c), and weak, diffuse *c* reflections. The streak geometry is identical to that found in Stillwater bytownites (Nord et al., 1974), and its trace measured in the [100] zone is 30° from b^* (toward $-c^*$) at the position of the *b* reflection and parallel to $[02\bar{1}]^*$ at the outer tail. Occasionally an intensity maximum is present beyond the end of the streak, corresponding to an *e* satellite. Exsolution of an $I\bar{1}$ phase and an intermediate plagioclase occurred in the calcic portion of the reverse zoned rim. The lamellae (Fig. 9) range from 80 to 150 Å in width and assume orientations that have both $(03\bar{1})$ and $(01\bar{1})$ components. Zig-zag *b* antiphase boundaries are present in the two-phase mixture and have contrast characteristics similar to the An_{80} Ardnamurchan plagioclase.

3.4. Warwick Plagioclase

Warwick metamorphic plagioclase contains three chemically distinct textural regions (see Appendix); optically homogenous intermediate plagioclase that varies from An_{62} to An_{66} in bulk composition, an optically visible two-phase intergrowth (An_{71} to An_{75}) and optically homogeneous bytownite (An_{85} to An_{88}). The orientation of exsolution lamellae was determined with the universal stage and the two exsolution directions were confirmed as $(03\bar{1})$ and $(30\bar{1})$. Occasionally $(03\bar{1})$ lamellae pass through albite twin boundaries with no deviation, a phenomenon that has been observed by Laves (1974). The compositions of the coexisting phases were estimated from refinement of lattice parameters and from measurements of the volume proportions of each phase in electron micrographs. Unit cell parameters for the sodic intermediate plagioclase and the calcic phase were determined by back-reflection Weissenberg techniques on a single crystal that contained optically visible two-phase intergrowths, and the results are consistent with compositions of An_{65} for the sodic phase and An_{85} for the calcic phase (Table 1). It should be noted that cell dimensions may not give reliable compositions for the two phases, since strain effects resulting from coherent exsolution often alter the lattice parameters. δh, δk and δl values obtained for s of the intermediate plagioclase phase compare well with those obtained by Gay (1956) for An_{64-67}. Transmission electron microscope observations indicate that optically homogeneous An_{62-67} plagioclase is a single phase on the scale of the TEM, but optically homogeneous calcic plagioclase (An_{85-88}) contains submicroscopic lamellae of intermediate plagioclase constituting 4 to 12 volume %. Using An_{66} as the composition of sodic lamellae, and An_{85} as the bulk composition the limits obtained for the calcic phase are An_{86} to An_{88} (with bulk composition of An_{88} the limits would be An_{89} to An_{91}). The composition estimates are consistent with those obtained by Cliff et al. (1976).

TEM Observations of Warwick Plagioclase

The optically homogeneous intermediate plagioclase and the two-phase intergrowths were described by Grove (1976), but recent observations merit further discussion. McConnell (1974) and Grove noted that superlattice fringes sometimes terminate doubly (see Grove's Figs. 1c, 2a). Intermediate plagioclase has a periodic antiphase structure, and each superlattice fringe represents an antiphase boundary. Thus, at a pair of terminating fringes the antiphase relation that is generated can be compensated by a 180° bend in the periodic APB. Such curved antiphase boundaries have been observed in the periodic antiphase structures of the Cu-Au alloys (Glossop and Pashley, 1959; Pashley and Presland, 1959). Curved APBs are also found at the boundary between intermediate plagioclase and $(03\bar{1})$ bytownite lamellae (Fig. 10a). At the interface between lamellae and host the periodic antiphase domains in the intermediate plagioclase are alternately out-of-phase or in-phase with the $(03\bar{1})$ calcic lamella at the host-lamellar boundary. Periodic APBs terminate at the host-lamellar boundary

Table 1. Values of $s = \delta h a^* + \delta k b^* + \delta l c^*$ measured from X-ray single-crystal oscillation photos. $d_{2s} = 1/(2|s|)$ is the periodicity of the periodic antiphase boundaries

Composition	δh	δk	δl	d_{2s}
Warwick plagioclase				
$An_{75.7}$	0.031	0.092	0.165	37.2
	0.030	0.090	0.153	39.7
	± 0.016[a]	± 0.019[a]	± 0.020[a]	
Nain gabbro				
$An_{67.4}$	0.025	0.077	0.098	56.1

Cell dimensions of plagioclase from two-phase intergrowth of Warwick plagioclase

	Intermediate phase	Calcic phase
a	8.1781 (6)[b]	8.1812 (12)
b	12.8683 (6)	12.8680 (8)
c	14.2046 (10)	14.1868 (18)
α	93.487 (7)	93.234 (9)
β	116.146 (5)	116.013 (8)
γ	90.330 (8)	90.970 (11)
V in Å^3	1338.54 (24)	1338.64 (40)
Number of observations	156	130

Bulk chemical analysis by electron microprobe An = 75.7, Or = 0.1

SiO_2	48.39
Al_2O_3	32.73
FeO	0.00
CaO	15.94
K_2O	0.01
Na_2O	2.87
Sum	99.95

[a] Errors estimated from uncertainty in oscillation photo measurements of Warwick plagioclase

[b] Parenthesized units represent the estimated standard deviation in terms of the least units cited. Therefore, 8.1781 (6) means 8.1781 ± 0.0006

in pairs, except where a single periodic antiphase boundary extends into the calcic lamella and becomes an antiphase boundary separating portions of the calcic lamella (at s in Fig. 10b). On opposite sides of the zig-zag APB the antiphase relations between calcic lamella and intermediate plagioclase domains are switched, and the periodic antiphase domains that were in-phase on one side of the zig-zag are out-of-phase with the calcic lamella on the other.

Textures of the plagioclase intergrowths observed near [100] show that $(03\bar{1})$ bytownite lamellae contain in addition to zig-zag antiphase boundaries a second set of intermediate plagioclase lamellae similar to those observed by Cliff et al. (1976). Previously the second generation of lamellae were only found in the $(30\bar{1})$ calcic lamellae by Grove (1976). The intermediate plagioclase lamellae included within $(03\bar{1})$ lamellae consistently display an orientation and periodicity

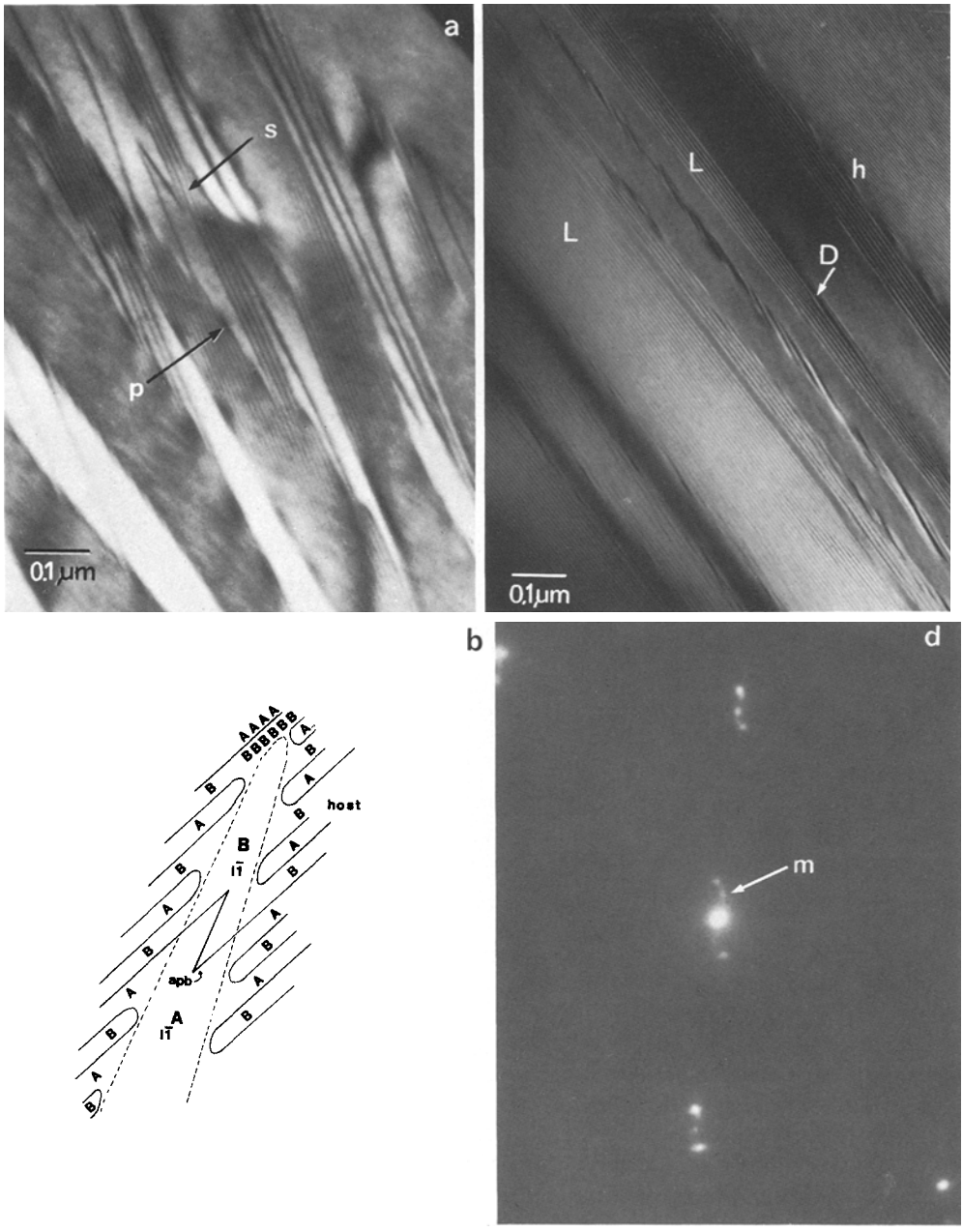

Fig. 10a–d. *Warwick plagioclase.* **a** Electron micrograph shows $(03\bar{1})$ calcic lamellae and intermediate plagioclase host. Periodic antiphase boundaries terminate in pairs (*p*) at the host-lamella boundary or extend into the calcic lamella to form an antiphase boundary (*s*). DF, $g=013$, $s=0$ for *e* satellite pair. **b** Schematic diagram of antiphase relations between intermediate plagioclase and $(03\bar{1})$ calcic lamella. The antiphase relations are represented by designating each antiphase domain as an *A* or *B* type. *B* is related to *A* by the *APB* fault vector. Solid lines depict the APBs, and the dashed lines the host-lamellar boundary. **c** Electron micrograph of intermediate plagioclase and $(03\bar{1})$ lamellae. Superlattice periodicity and orientation changes locally. Fringes in lamella (*L*) are rotated 6 degrees with respect to fringes in the host (*h*). Superlattice fringes terminate in pairs at (*D*). DF, $g=\bar{2}02$, $s=0$ for *a* and *f* reflection. **d** Enlargement of electron diffraction pattern taken in region of (**c**). An *a–f* pair (center) and two *b–e* pairs are shown. Streak between the *a* and *f* reflection with a maximum along its length (*m*) suggests an intermediate plagioclase with an orientation and periodicity different from the host. [111] zone

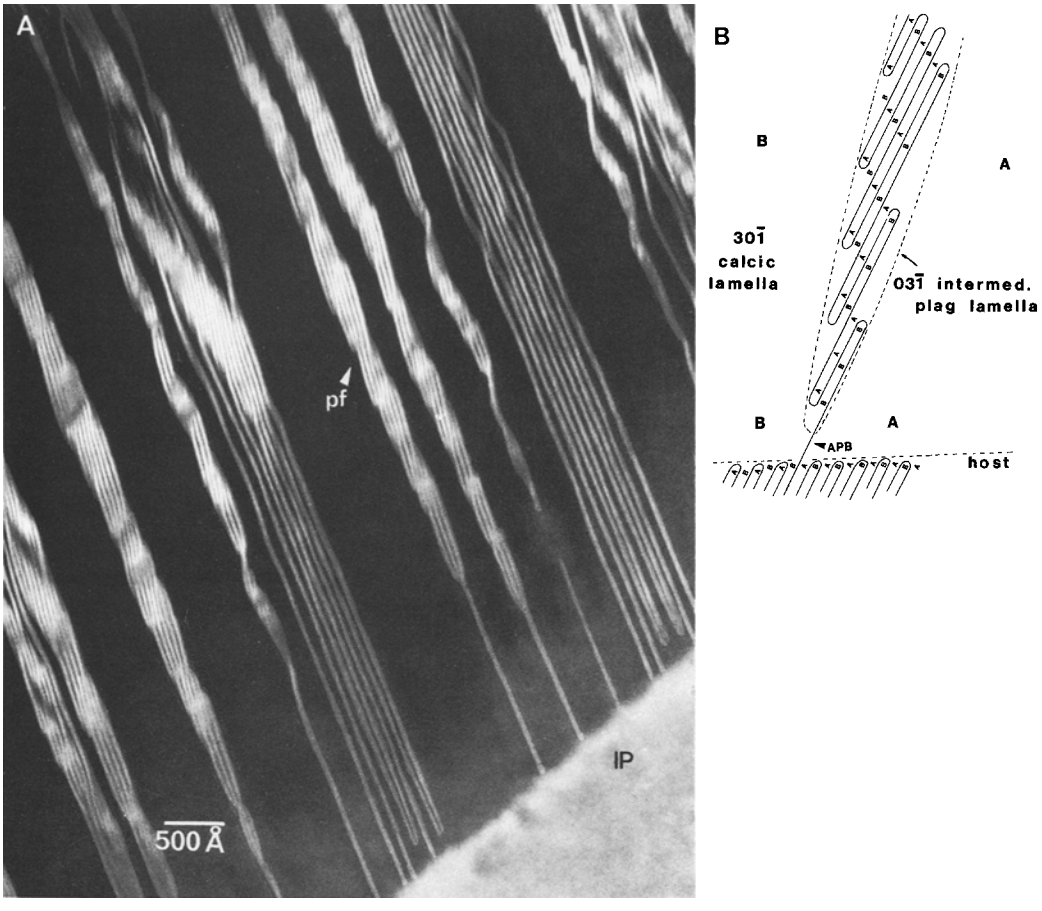

Fig. 11A and B. A Electron micrograph of a (30$\bar{1}$) calcic exsolution lamella containing second generation lamellae parallel to (03$\bar{1}$) (*pf*). Intermediate plagioclase host (*IP*) is at lower right. DF, $g=(1\bar{6}3)$, $s=0$ for *e* satellite pair. Published in Exsolution in Metamorphic Bytownite. In: Electron Microscopy in Mineralogy (H.R. Wenk et al., eds.), Berlin: Springer 1976. **B** Illustration of the antiphase relations for the second generation (03$\bar{1}$) intermediate plagioclase lamella. Every other periodic antiphase domain within the intermediate plagioclase lamella bears an out-of-phase relation to the (30$\bar{1}$) calcic lamella. *A* curved *APB* is present to compensate for the mismatch

that differs from that of the host phase (Fig. 10c). The difference in orientation is approximately 6° while the periodicity increases by approximately 40%. The change in orientation and periodicity is also apparent in (03$\bar{1}$) lamellae within the (30$\bar{1}$) calcic lamellae (Fig. 11a). Streaking visible in diffraction patterns between *b–e* and *a–f* pairs (Ribbe, 1975) suggests the presence of small oriented platelets of intermediate plagioclase and the TEM observations confirm that although the (03$\bar{1}$) lamellae are optically visible, on the submicroscopic scale they consist of intergrown bytownite and second generation intermediate plagioclase which vary in orientation and periodicity. Sometimes a maximum is present

along the streaks between *a–f* reflection pairs (Fig. 10d) confirming the presence of intermediate plagioclase with different orientation and periodicity.

An interpretation of the interface relations between a $(03\bar{1})$ intermediate plagioclase lamella within a $(30\bar{1})$ calcic lamella is pictured in Figure 11b. The single fringes that extend from the base of the $(03\bar{1})$ lamellae into the intermediate plagioclase host are antiphase boundaries. Therefore, the portions of the $(30\bar{1})$ calcic lamella on either side are in antiphase relation and the periodic antiphase domains of the $(03\bar{1})$ intermediate plagioclase lamella that are in-phase on one lamellar-host interface are out-of-phase at the other, requiring a switchback arrangement of antiphase boundaries to satisfy the antiphase relations. Note that the orientation and periodicity of superlattice fringes change within a single included lamella consistent with the streaking observed between *b–e* reflection pairs.

TEM Observations in Calcic Regions (An_{85-88})

Warwick plagioclase with bulk composition An_{85} to An_{88} consists of a two-phase intergrowth in which $I\bar{1}$ calcic plagioclase predominates (Fig. 12), and $(03\bar{1})$ intermediate plagioclase is present as sparse lamellae from 0.05 to 0.1 microns wide. Between the lamellae are long, straight antiphase boundaries and smaller inclusions of intermediate plagioclase that range from 2 to 10 periodic antiphase domains in thickness (Fig. 12b, c). The relations between the periodic antiphase domains of intermediate plagioclase and the calcic $I\bar{1}$ phase are as expected for a periodic antiphase structure, the periodic APBs within the intermediate plagioclase lamellae either terminate by a 180° curved APB or extend as single antiphase boundaries into the calcic phase.

4.1. Discussion: Structural Characterization

The TEM observations can now be combined with the estimates of the cooling history for the 4 geologic environments to give a structural characterization of labradorite-bytownite plagioclase. The structural characterization is made by inferring the transformation-exsolution sequence that a particular plagioclase undergoes as a function of cooling history, and it is based on the interpretation of TEM textures. Three important assumptions are made; (1) the presence of *b* antiphase boundaries in the igneous plagioclases implies a $C\bar{1}$ to $I\bar{1}$ transformation, (2) the wormy intergrowth of intermediate plagioclase domains resulted from a $C\bar{1}$ to intermediate plagioclase transformation, and (3) the lamellar modulation is related to the formation of short-range ordered domains with $P\bar{1}$-like symmetry. Exsolution textures coarsen with prolonged annealing times and are arbitrarily divided into 2 groups; those that are optically visible under 500 × magnification and those that are discernible only in the TEM. The structural characterization is summarized for each sample on a cooling rate vs. composition plot (Fig. 13). The figure shows the structural transformations that occur for a particular bulk composition, and samples are arranged according

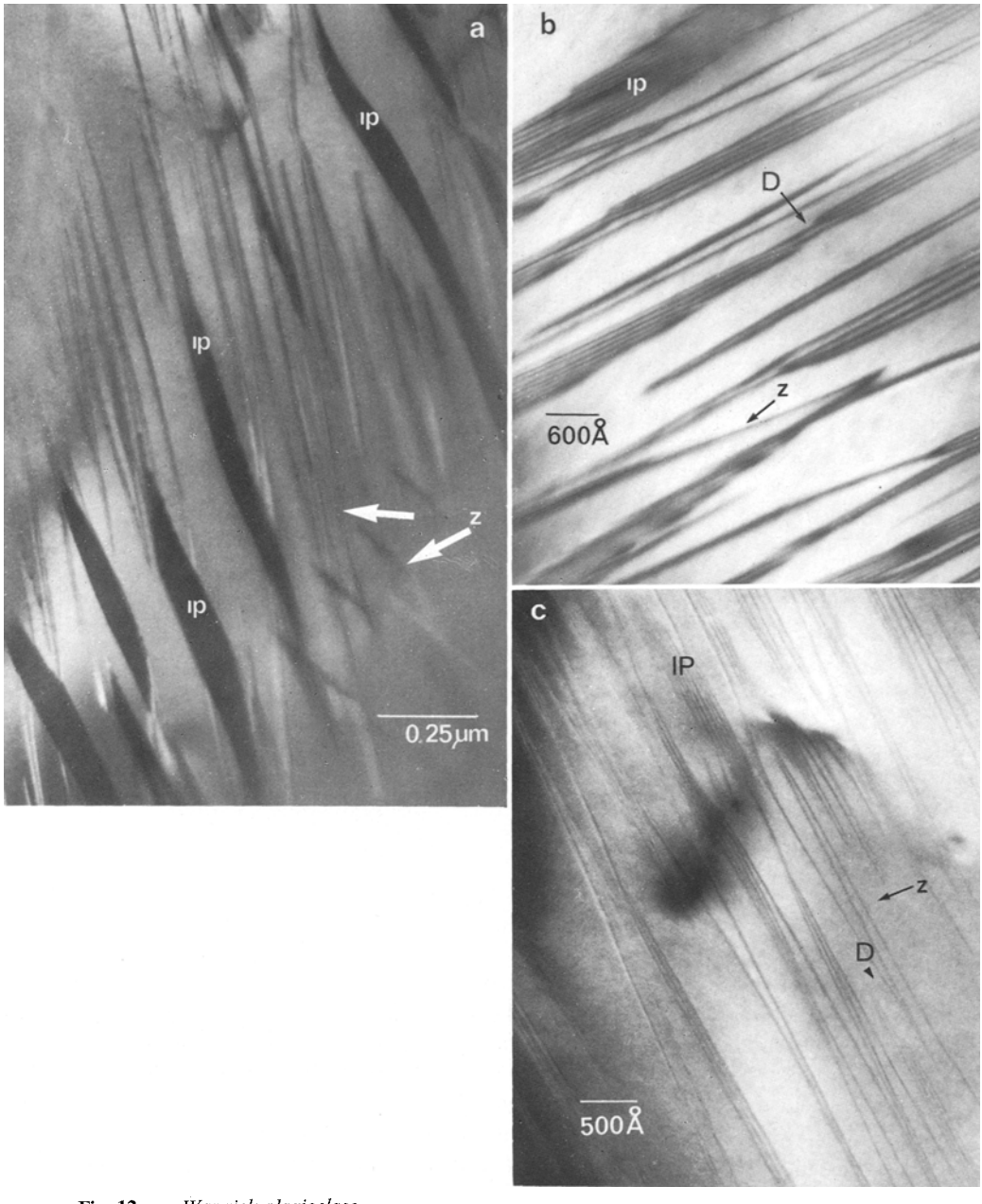

Fig. 12a–c. *Warwick plagioclase*
a Electron micrograph of calcic region (An_{85-88}). Intermediate plagioclase ($03\bar{1}$) lamellae (*IP*) are surrounded by the $I\bar{1}$ calcic phase. Within the calcic phase are antiphase boundaries (*z*) and small regions of intermediate plagioclase (*IP*). DF, $g=031$, $s=0$ for *b* reflection. **b** Electron micrograph of calcic region. Periodic antiphase boundaries of intermediate plagioclase ($03\bar{1}$) lamellae terminate in pairs (*D*) or extend singly into $I\bar{1}$ calcic phase to create antiphase boundaries (*z*). DF, $g=013$, $s=0$ for *b* reflection and *e* satellite pair. **c** Electron micrograph of calcic region in which $I\bar{1}$ phase predominates. Intermediate plagioclase lamellae (*IP*) consist of three to six periodic antiphase domains and a zig-zag antiphase boundary can be traced at (z). DF, $g=01\bar{1}$, $s=0$ for *b* and *e* satellite pair

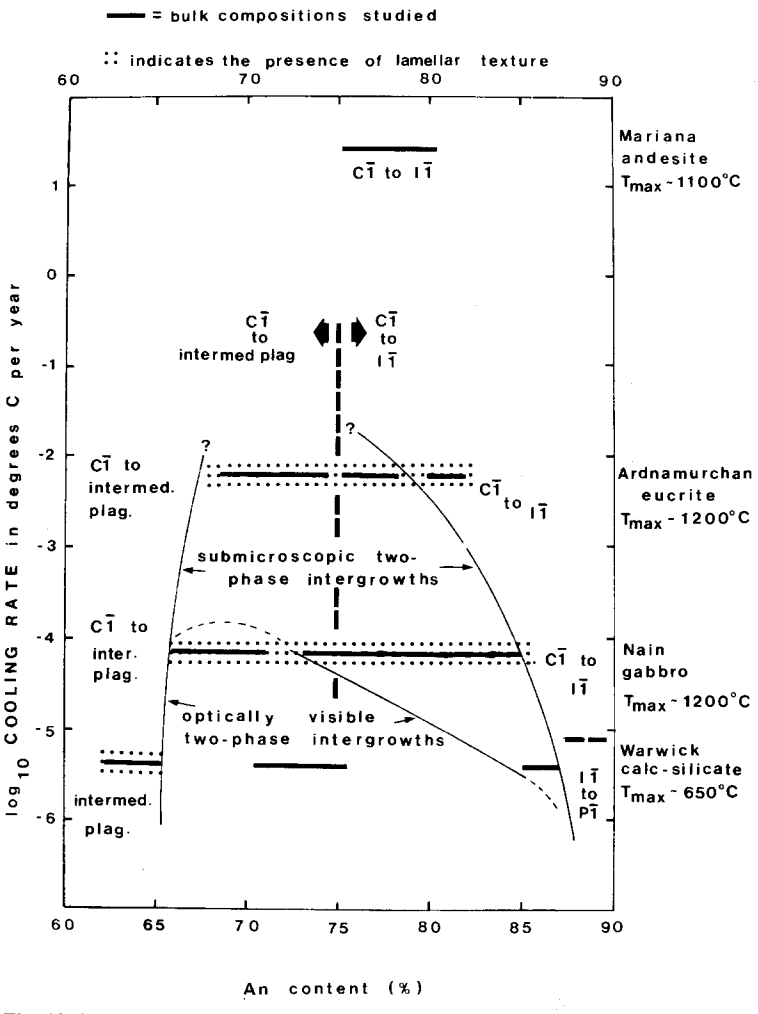

Fig. 13. Structural transformation sequence for the plagioclase samples inferred from TEM observations. The geologic environments are arranged according to time-integrated cooling rate and the exsolution-transformation sequence is indicated for the bulk compositions (solid horizontal lines) studied. Lamellar texture is related to diffuse *c* reflections

to cooling rate. In addition, the maximum estimated temperature indicates that the cooling histories of the igneous plagioclases started at similar temperatures (1100–1200° C), while the cooling history of the Warwick plagioclase was initiated at a much lower temperature (650° C).

4.2. Exsolution Textures

The most striking effect of cooling history is on the compositional range of exsolution. For the most rapidly cooled plagioclase, no evidence of exsolution is present. With progressively slower cooling the compositional range of two-

phase intergrowths increases. All samples show exsolution in labradoritic compositions (as sodic as An_{77}), and the effect of slower cooling is that exsolution occurs in increasingly more calcic bulk compositions. Also, for an equivalent cooling history the lamellae in sodic bulk compositions grow to a larger size than those in the calcic bulk compositions, suggesting that greater proportions of Ca and Al impede the unmixing process. The bulk composition limits for exsolution are shown in Figure 13 (light lines), but the composition of coexisting plagioclases cannot be inferred from the diagram. In all plagioclases studied there is evidence for local disequilibrium. The calcic lamellae in Warwick and Nain plagioclase contain second-generation intermediate plagioclase lamellae, and the intermediate plagioclase of Ardnamurchan two-phase intergrowths varies in composition on the submicroscopic scale. Hence, the coexisting plagioclases cover a range of compositions; the intermediate plagioclase varying on a submicroscopic scale and the calcic lamellae becoming more calcic by exsolving a second generation of compositionally distinct intermediate plagioclase.

The exsolution textures in the rapidly cooled plagioclases consist of stringy lamellae 50 to 100 Å wide that vary from being parallel to $(03\bar{1})$ to the orientation of the periodic antiphase boundary of the intermediate phase. This type of morphology is retained for the slowly cooled specimens, but the lamellar size increases and lamellae density decreases. Lamellae in the Warwick and Nain plagioclase retain the variation in orientation. The widths increase to 0.2 to 0.5 micron and a second exsolution direction parallel to $(30\bar{1})$ develops.

4.3. The $C\bar{1}$ to $I\bar{1}$ Transition

The sodic compositional limit for the $C\bar{1}$ to $I\bar{1}$ transformation is inferred as An_{75}, (dashed vertical line on Fig. 13) from the presence of *b* antiphase domains in both igneous and volcanic plagioclase. Hydrothermal annealing experiments performed by McConnell (1974) on two-phase intergrowths (An_{75}) from the Stillwater and Bushveldt igneous intrusives resulted in the disappearance of intermediate plagioclase while $I\bar{1}$ plagioclase remained, suggesting that the exsolution temperature is below the $C\bar{1}$ to $I\bar{1}$ inversion temperature. The sodic limit of An_{75} for the $C\bar{1}$ to $I\bar{1}$ transition is also suggested by the observations of McLaren and Marshall (1974) in Lake County labradorite (their Fig. 2). The textures in Lake County bear a striking resemblance to those observed in An_{68} to An_{74} Ardnamurchan plagioclase, and are quite different from the smoothly curving *b* antiphase boundaries found in the Mariana plagioclase (Fig. 3).

Heuer and Nord (1976a) point out that antiphase domain morphology in calcic plagioclase can be a useful indicator of cooling history, and it appears to be the case for An_{75} to An_{85} plagioclase. Compare the antiphase boundary morphology in Mariana plagioclase (An_{80}, Fig. 3) to that in Ardnamurchan An_{80} (Fig. 7) and calcic Nain plagioclase (Fig. 9). The rapidly cooled specimen contains curved, smooth boundaries, but with increased annealing time the boundaries orient themselves with respect to crystallographic planes. Nord et al. (1974) suggest that the change in antiphase boundary morphology may be related

to the approach of antiphase boundary orientations to low-energy crystallographic planes. However, the interaction of exsolution lamellae and antiphase boundaries may also play a role in antiphase boundary morphology.

The antiphase boundaries found in the calcic lamellae of Warwick plagioclase (Figs. 10a, 11a) are related to the periodic antiphase structure of the host. Nucleation of the calcic phase may occur in several parts of the intermediate plagioclase host and it is highly probable that the $I\bar{1}$ calcic lamellae will grow into antiphase relations with one another. Similarly, the presence of antiphase boundaries and periodic APBs in the An_{85} Warwick plagioclase (Fig. 12) may be accounted for by the interaction of the intermediate plagioclase and the $I\bar{1}$ host and possibly by presence of dislocation-generated antiphase boundaries. The highest temperature experienced by the metamorphic plagioclase was about 650°C, which is below the temperature of the $C\bar{1}$ to $I\bar{1}$ transition making it unlikely that the antiphase boundaries found in the Warwick plagioclase are thermal in origin.

4.4. Defects Structures of Intermediate Plagioclase

Several authors have puzzled over the texture observed in intermediate plagioclase (Wenk et al., 1975; McLaren and Marshall, 1974; Hashimoto et al., 1976) that are described here as wormy intergrowths. My observations indicate that two-phase intergrowths are associated in the Ardnamurchan and Nain plagioclase with the texture, but it is not necessary that an $I\bar{1}$ phase and an intermediate plagioclase be present for the wormy texture to appear. The wormy texture is present in An_{66} Warwick plagioclase (Grove, 1976, Fig. 1d), in Wenk et al.'s metamorphic plagioclase (their Fig. 6a) and in McLaren and Marshall's An_{32} plagioclase (their Fig. 7) where there is no evidence for an $I\bar{1}$ phase. As pointed out by Wenk et al., the contrast from the wormy intergrowth is not characteristic of antiphase boundaries, and their explanation that the texture is related to structural mistakes in the superstructure is probably correct. It is difficult to characterize the precise nature of the defect, because it is related to the periodic antiphase structure and is not an ordinary stacking fault or dislocation, but it probably results from a mismatch between the periodic antiphase structure of 2 domains of intermediate plagioclase.

The images observed in Nain An_{72} and Ardnamurchan An_{68-74} plagioclase (Figs. 8b, 5) are probably dominated by overlapping domains of intermediate plagioclase, but these domains (as evidenced by Fig. 5b) are separated by thin $I\bar{1}$ lamellae. Whatever the nature of the texture it appears to be a useful indicator of cooling history, since it becomes pregressively coarser with slower cooling rates.

4.5. Transformation Sequence in Intermediate Plagioclase

There has been some speculation that the intermediate plagioclase transformation sequence on cooling is $C\bar{1}$ to $I\bar{1}$ followed by an $I\bar{1}$ to intermediate plagioclase transition. Since the structure of each periodic antiphase domain of intermediate

plagioclase is consistent with $I\bar{1}$, such a complex transition process is not necessary. A method of growing intermediate plagioclase consistent with McLaren and Marshall's (1974) observation on An_{66} (their Fig. 2) is the formation of $I\bar{1}$-like domains (accompanied by diffuse *b* reflections) that order into periodic antiphase domains. The differences between submicroscopic textures observed in An_{65}-An_{75} and An_{75}-An_{85} indicate that the transformation sequence is different in sodic bulk compositions from that in the more calcic plagioclase. Hence, the existence of a discreet $I\bar{1}$ phase is not necessary and it is perhaps easier to think of the transformation as $C\bar{1}$ to intermediate plagioclase.

Compositional Limits of the Intermediate Plagioclase Structure

It is rather difficult to define a calcic compositional limit for intermediate plagioclase, since any plagioclase of bulk composition An_{66} to An_{85} may contain an intermediate plagioclase. The study of the Warwick plagioclase suggests that An_{66} is the equilibrium composition. The TEM observations of the igneous rocks imply that plagioclase with bulk composition to An_{75} undergoes a transformation from $C\bar{1}$ to intermediate plagioclase and exsolves to form coexisting intermediate plagioclase and $I\bar{1}$ plagioclase. Plagioclase more calcic than An_{75} undergoes a $C\bar{1}$ to $I\bar{1}$ transition and also unmixes to form an intermediate plagioclase and an $I\bar{1}$ intergrowth. Thus, An_{66} is the limit for a single-phase intermediate plagioclase, and more calcic compositions consist of $I\bar{1}$ and intermediate plagioclase intergrowths in which the intermediate plagioclase takes on a range of orientations and periodicities.

4.6. Lamellar Modulation

This texture (also called cross-hatched texture, Wenk et al., 1973) is visible in dark field micrographs taken with *a* reflections in all plagioclases except for the Mariana plagioclase and the calcic lamellae of the Warwick two-phase intergrowths. The lamellar structure is distinct from the exsolution textures of $I\bar{1}$ and intermediate plagioclase intergrowths (compare Figs. 4 and 5), and it is found in specimens that show no evidence for two phases (e.g. An_{66} Nain, Fig. 8a, and An_{80} Ardnamurchan plagioclase). Diffuse streaks are observed in the position of *c* reflections (Fig. 4b) and may explain the origin of the lamellar modulation, since the streaks are approximately perpendicular to the orientation of sub-parallel dark and light striations observed in dark field micrographs (Fig. 4d). An interpretation consistent with McLaren's (1974) explanation for a similar texture observed in An_{75} and the diffraction pattern evidence is that the structure results from the presence of short-range ordered domains with $P\bar{1}$ symmetry. The absence of the lamellar modulation in Mariana plagioclase is consistent with the lack of *c* reflections, and the absence of the structure in Warwick bytownite is explained by the presence of discreet *c* antiphase domains and associated *c* and *d* reflections. A lamellar modulation is present in intermediate plagioclase (Fig. 8a), suggesting the formation of $P\bar{1}$-like

domains in the periodic antiphase structure. Cole et al. (1951) and Gay (1956) noted the presence of weak *c* reflections in X-ray diffraction patterns of intermediate plagioclase, and in recent X-ray structural studies, evidence for $P\bar{1}$-like domains has been found (Toman and Frueh, 1975a, b). One of the major differences between the $P\bar{1}$ and $I\bar{1}$ structures is the change of alkali atom position within the irregular tetrahedral framework hole, which also involves an adjustment of the tetrahedral framework to accomodate the alkali atom. Perhaps the adjustments occur in all plagioclase (even intermediate plagioclase) and cause the formation of domains that are $P\bar{1}$ in nature.

4.7. $An_{87.5}$ – the Calcic End Member of the Miscibility Gap

Cliff et al. (1976) used analytical microscopy to define the composition of the calcic member of Huttenlocher intergrowths as $An_{88\pm4}$, in close agreement with the results of this study. It is tempting to speculate that $An_{87.5}$ could be an ordered end member of the exsolution. If ordering occurred in the anorthite alkali sites such that one site contained Na and the other seven sites contained Ca, the $P\bar{1}$ symmetry of the structure would be destroyed and an ordered phase with P1 symmetry created. The diffraction geometry is consistent with $P\bar{1}$ or P1 (weak *c* and *d* reflections) and there may exist an ordered low-temperature form in the plagioclase series. Several lines of evidence suggest that the *c* and *d* reflections in anorthite result from more than a displacive transformation from $I\bar{1}$ to $P\bar{1}$. High-temperature studies of anorthite (Foit and Peacor, 1973) indicate an inability of the anorthite structure to attain truly $I\bar{1}$ symmetry at elevated temperatures. Heating stage studies of *c* antiphase boundaries in anorthite (Müller and Wenk, 1973) show that despite the disappearance of APBs on heating they reappear in the same place upon cooling. The antiphase boundaries can be destroyed only by long-term heat treatment at high temperature. These observations led Heuer et al. (1976b) to propose a two-step transformation for $P\bar{1}$ anorthite. Recent refinement of An_{90} from lunar sample 76535 (Smyth, 1976) indicates deviations of this plagioclase from centrosymmetry. Smyth observes preferential occupancy of one alkali site by Na and positional differences in the Ca sites that should be related by the inversion center.

5. Conclusions

This study of labradorite-bytownite plagioclase shows that Huttenlocher plagioclases are useful as indicators of cooling history. Most plagioclases found in nature are chemically zoned and a careful study of a single zoned plagioclase crystal can tell a great deal about the geologic history of its host rock. The TEM observations indicate that (1) the bulk-compositions in which Huttenlocher exsolution are observed depend on cooling history and the closest approach to equilibrium appears to consist of An_{66} and An_{85-90} intergrowths, (2) the size and morphology of exsolution lamellae are useful as indicators of cooling

history if the bulk composition of the plagioclase is known, (3) the morphology of *b* antiphase boundaries is useful in An_{75} to An_{85} plagioclase as cooling history indicators and (4) the wormy texture observed in intermediate plagioclase may serve as an indicator of cooling history. Because of the differences in textures observed in the TEM, it is suggested that the transformation sequence in plutonic samples for An_{75} to An_{85} differs from that for An_{66} to An_{75}. The presence of *b* antiphase boundaries and the lack of exsolution lamellae in rapidly cooled An_{75-85} plagioclase and the presence of both *b* APBs and exsolution in slowly cooled specimens is interpreted as a $C\bar{1}$ to $I\bar{1}$ transition followed by exsolution. The absence of *b* APBs and the presence of a wormy texture in the intermediate plagioclase member of An_{65}-An_{75} two-phase intergrowths is interpreted as a $C\bar{1}$ to intermediate plagioclase transition followed by exsolution. In the metamorphic plagioclase there is no compelling evidence that indicates a transformation sequence. It is inferred from the low temperature of formation that intermediate plagioclase and $I\bar{1}$ plagioclase were the stable structural forms under the existing conditions.

Appendix-Geologic History of Plagioclase and Calculation of Cooling History

The Mariana plagioclase was collected from andesite flows of the Tertiary Hagman formation in the Mariana Islands (sample MSS-3f of Schmidt, 1953). Plagioclase phenocrysts are zoned in an oscillatory manner from An_{90} cores to An_{74} rims. The sample of Ardnamurchan plagioclase came from the great eucrite of the Tertiary Ardnamurchan intrusive center in western Scotland (Richey and Thomas, 1930). Individual crystals are normally zoned from core composition of An_{87} to rims of calcic labradorite (An_{63}).

The Nain plagioclase sample was collected from a gabbro of the Precambrian layered Bridges Group of Paul Island, Labrador (Wheeler, 1960; Planansky, 1972; Berg, 1974). The sample studied (129-1 of Planansky) has plagioclase crystals with cores that vary from An_{62} to An_{70} and thin rims (0.25 to 0.5 mm) that are reverse zoned from An_{72} to An_{85} (Fig. 14a). The triangles of Figure 14a indicate bulk electron microprobe analyses of regions in which a two-phase intergrowth is optically visible (An_{66} to An_{70}). The reverse zoned calcic rims appear optically to consist of one phase.

The Ordovician Partridge formation yielded the Warwick plagioclase. The specimen (F-34 of Robinson, 1963) is a calc-silicate collected in Warwick, Massachusetts from sillimanite-grade metamorphic rocks. The compositional variations within plagioclase grains are complex. Individual grains are reverse zoned from cores of An_{62} to rims of An_{88} (Fig. 14b). The sodic cores are optically homogeneous labradorite (An_{62} to An_{66}) rimmed by a two-plagioclase intergrowth with bulk composition An_{71} to An_{75} (triangles in Fig. 14b). Narrow rims of optically homogeneous bytownite (An_{85}-An_{88}) surround the two-phase intergrowths. Similar plagioclases have been described by Nissen (1974) from Valle d'Ossa, Italy. Some grains contain regions of homogeneous bytownite or patches that consist of the two-phase intergrowth. These patches are surrounded by homogeneous labradorite.

Calculation of Cooling Histories

Lovering (1935) solved the heat equation for a variety of intrusive bodies including a dike or sill, an extrusive sheet and a laccolith (spherical approximation). The assumptions of Lovering's model for heat conduction in igneous intrusives are many, and these calculations are only intended to be estimates of cooling rate. The boundary conditions required for Lovering's calculation are found in Table 2 and the assumptions used in setting the conditions are briefly summarized below.

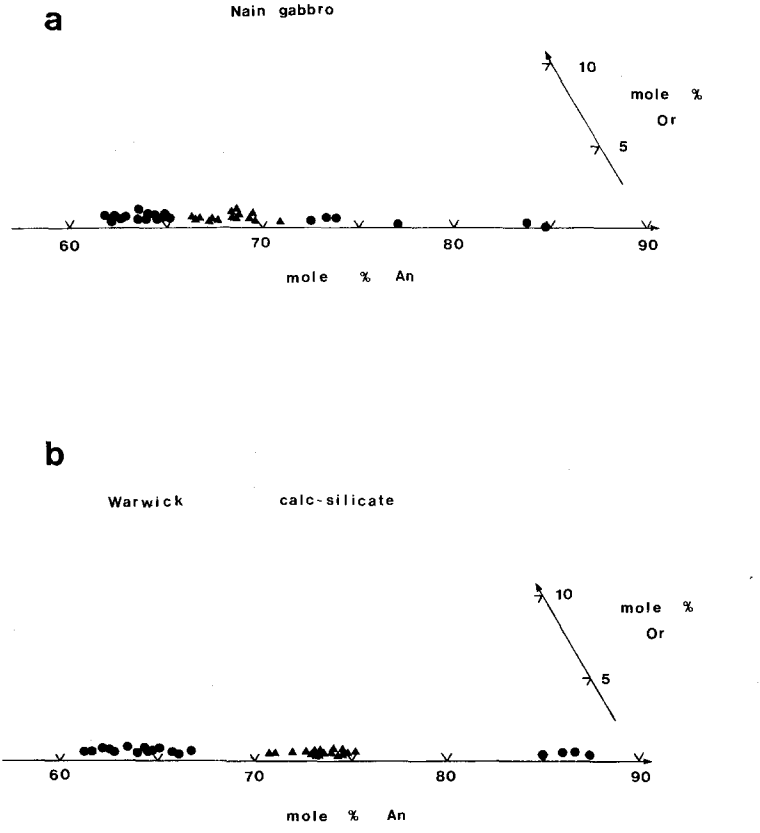

Fig. 14. a Electron microprobe analyses of plagioclase from Nain gabbro. **b** Electron microprobe analyses of Warwick plagioclase. Circles indicate an analysis of an area that appears to be optically homogeneous at 500 ×. Triangles indicate a bulk analysis of an area that appears to be a two-phase intergrowth

Table 2. Boundary conditions used in the solution of the heat equation

Cooling history assumptions	Mariana Islands	Ardnamurchan	Nain
Initial temperature	1100° C	1200° C	1200° C
Wall rock temperature	0° C	100° C	500° C
Shape of intrusive/extrusive	Extrusive sheet	Sill and laccolith	Sill, calculated for two thicknesses
Size of intrusive/extrusive (in meters)	10 to 30 m thick	2500 m thick and 2500 m radius	Varied between 6000 and 10,000 m
Position of sample in intrusive (in meters)	Center	1250 m from edge of sill and center of sphere	2000 m from base

The value of diffusivity given by Jaeger (1957) for basalt magma (0.006) was used for all calculations.

The initial temperatures for the Ardnamurchan and Nain intrusives were assumed to be 1200° C, because both rocks appeared to have liquid coexisting with olivine, plagioclase and pyroxene (Walker et al., 1973; Roeder and Osborn, 1966) and bulk Fe/(Fe+Mg) of 0.3. Since the Mariana andesite was saturated with plagioclase, pyroxene and silica during its crystallization and has higher bulk Fe/(Fe+Mg) ($\sim$0.5) the initial temperature was taken at 1100° C. Wall rock temperatures were estimated from the depth of burial, assuming a 30° C/km geothermal gradient. The sample localities were used to determine the position in the body for which the heat equation was solved.

Warwick Calc-Silicate

The cooling history of the regionally metamorphosed Warwick calc-silicate was calculated by estimating the change in temperature associated with erosion and uplift of the buried metasediment. The initial temperature and pressure are taken as that recorded by the metamorphic mineral assemblage (650° C and a pressure of 6 kilobars (Robinson and Jaffe, 1969). Robinson (1966) proposes an overburden of 30 km of sediments from reconstruction of folded structures in the Orange area, Massachusetts, and calculates erosinal rates from structural considerations, ranging from 73 to 7 cm/1000 years for the time period middle Devonian (or Permian) to Triassic. The time-temperature paths in accordance with the erosional rates of Robinson (the ranges are chosen between 100 cm/10^3 yr and 10 cm/10^3 yr) and a geothermal gradient of 20° C/km (Birch et al., 1968) are plotted in Figure 3. This approximation can be checked by comparison of cooling rate estimates in other regional metamorphic environments. Hunziker (1970) and Jäger et al. (1967) have determined cooling rates from K-Ar retention ages in biotites and muscovites from regionally metamorphosed rocks in the Alps. Their estimates (2×10^{-5} °C/yr) are in close agreement with the rates estimated from erosion of 2×10^{-5} to 2×10^{-6} °C/yr.

Acknowledgments. The author thanks C.W. Burnham, J.B. Thompson, Jr., J.F. Hays, G.L. Nord, Jr., and J.D.C. McConnell for stimulating discussions on the plagioclases. David Kohlstedt and John van der Sande of M.I.T. assisted patiently in the transmission electron microscopy, and Chris Goetze generously provided access to M.I.T.'s ion thinner. Financial support for this study was provided by the National Science Foundation Grants #GA12852 and GA41415 to C.W. Burnham

References

Berg, J.H.: Paleogeobarimetric map of the Nain Complex (S.A. Morse, ed.), The Nain Anorthosite Project, Labrador: Field Report 1974, Contr. **17**, pp. 34–36; Geology Department, University of Massachusetts, Amherst, Massachusetts (1974)

Birch, F., Roy, R., Decker, E.: Heat flow and thermal history in New England and New York. In: Studies of appalachian geology, Northern and Maritime (E-an Zen, W.S. White, J.B. Hadley, and J.B. Thompson, Jr., eds.), pp. 437–451. New York: Wiley Interscience 1968

Booth, M., Gittos, M., Wilkes, P.: A general program for interpreting electron diffraction patterns. 10 pp. Department of Metallurgy, University of Manchester 1973

Bown, M.G., Gay, P.: The reciprocal lattice geometry of the plagioclase feldspar structures. Z. Krist. **111**, 1–14 (1958)

Cliff, G., Champness, P.E., Nissen, H.-U., Lorimer, G.W.: Analytical electron microscopy of exsolution lamellae in plagioclase feldspars. In: Electron microscopy in mineralogy (H.R. Wenk et al., eds.), pp. 258–265. Berlin-Heidelberg-New York: Springer 1976

Cole, W.F., Sørum, H., Taylor, W.H.: The structures of the plagioclase feldspars. I. Acta Cryst. **40**, 20–29 (1951)

Foit, F.F., Jr., Peacor, D.R.: The anorthite crystal structure at 410° and 830° C. Am. Mineralogist **58**, 665–675 (1973)

Gay, P.: The structures of the plagioclase feldspars. III. Mineral. Mag. **30**, 169 (1953)

Gay, P.: The structures of the plagioclase feldspars: VI. Natural intermediate feldspars. Mineral. Mag. **31**, 21–40 (1956)

Glossop, A.B., Pashley, D.W.: The direct observation of anti-phase domain boundaries in ordered copper-gold (CuAu) alloy. Proc. Roy, Soc. (London), Ser. A**250**, 132–146 (1959)

Grove, T.L.: Exsolution in metamorphic bytownite. In: Electron microscopy in mineralogy (H.R. Wenk et al., eds.), pp. 266–270. Berlin-Heidelberg-New York: Springer 1976

Hashimoto, H., Nissen, H.-U., Ono, A., Kumao, A., Endoh, H., Woensdregt, C.F.: High resolution electron microscopy of labradorite feldspar. In: Electron microscopy in mineralogy (H.R. Wenk et al., eds.), pp. 332–344. Berlin-Heidelberg-New York: Springer 1976

Heuer, A.H., Lally, J.S., Christie, J.M., Radcliffe, S.V.: Phase transformations and exsolution in lunar and terrrestrial calcic plagioclases. Phil. Mag. **26**, 465–482 (1972)

Heuer, A.H., Nord, G.L., Jr.: Polymorphic phase transitions in minerals. In: Electron microscopy in mineralogy (H.R. Wenk et al., eds.), pp. 274–303. Berlin-Heidelberg-New York: Springer 1976a

Heuer, A.H., Nord, G.L., Jr., Lally, J.S., Christie, J.M.: Origin of the (c) domains of anorthite. In: Electron microscopy in mineralogy (H.R. Wenk et al., eds.), pp. 345–353. Berlin-Heidelberg-New York: Springer 1976b

Hirsch, P.B., Howie, A., Nicholson, R.B., Pashley, D.W., Whelan, M.J.: Electron microscopy of thin crystals. 549 pp. London: Butterworth 1965

Hunziker, J.C.: Polymetamorphism in the Monte Rosa, western Alps. Eclogae Geol. Helv. **63**, 151–161 (1970)

Huttenlocher, H.: Beiträge zur Petrographie des Gesteinzuges Ivrea Verbano. I. Allgemeines. Die gabbroiden Gesteine von Anzola. Schweiz. Mineral. Petrog. Mitt. **22**, 326–366 (1942)

Jäger, E., Huttenlocher, H.: Beobachtungen an basischen Plagioklasen der Ivrea-Zone. Schweiz. Mineral. Petrog. Mitt. **35**, 199–207 (1955)

Jäger, E., Niggli, E., Wenk, E.: Rb-Sr Altersbestimmungen an Glimmer der Zentralalpen. Beitr. Geol. Karte Schweiz, 67 pp. (1967)

Jaeger, J.C.: The temperature in the neighborhood of a cooling intrusive sheet. Am. J. Sci. **255**, 306–318 (1957)

Landuyt, J. van, Gevers, R., Amelinckx, S.: Fringe patterns at antiphase boundaries with $\alpha = \pi$ observed in the electron microscope. Phys. Stat. Sol. **7**, 519–546 (1964)

Laves, F.: Domain and deformation textures in plagioclases and their investigation by photoemission electron microscopy (PEEM) and by transmission electron microscopy. In: The feldspars (W.S. Mackenzie and J. Zussman, eds.), pp. 536–550. Manchester: Manchester University Press 1974

Laves, F., Goldsmith, J.R.: Short-range order in anorthite. Am. Cryst. Assoc. Meeting, Chicago (Abs., p. 10) 1951

Lovering, T.S.: Theory of heat conduction applied to geologic problems. Geol. Soc. Am. Bull. **46**, 69–93 (1935)

Marcinkowski, M.J.: Theory and direct observation of antiphase boundaries and dislocations in superlattices. In: Electron microscopy and strength of crystals (G. Thomas and J. Washburn, eds.), pp. 333–440. New York: Interscience Publishers 1963

McConnell, J.D.C.: Analysis of the time-temperature transformation behavior of the plagioclase feldspars. In: The feldspars (W.S. MacKenzie and J. Zussman, eds.), pp. 460–477. Manchester: Manchester University Press 1974

McConnell, J.D.C., Fleet, S.G.: Direct electron optical resolution of antiphase domains in a silicate. Nature **199**, 586 (1963)

McLaren, A.C.: Transmission electron microscopy of the feldspars. In: The feldspars (W.S. Mac Kenzie and J. Zussman, eds.), pp. 378–423. Manchester: Manchester University Press 1974

McLaren, A.C., Marshall, D.B.: Transmission electron microscope study of the domain structures associated with the b-, c-, d-, e-, and f-reflections in plagioclase feldspars. Contrib. Mineral. Petrol. **44**, 237–250 (1974)

Müller, W.F., Wenk, H.-R., Thomas, G.: Structural variations in anorthites. Contrib. Mineral. Petrol. **34**, 304–314 (1972)

Müller, W.F., Wenk, H.-R.: Changes in the domain structures of anorthites induced by heating. Neues Jahrb. Mineral. Monatsh., pp. 17–26 (1973)

Müller, W.F., Wenk, H.-R., Bell, W.L., Thomas, G.: Analysis of the displacement vectors of antiphase domain boundaries in anorthites ($CaAl_2Si_2O_8$). Contrib. Mineral. Petrol. **40**, 63–74 (1973)

Nissen, H.-U.: A study of bytownites in amphibolites of the Ivrea-Zone (Italian Alps) and in anorthosites: A new unmixing gap in the low plagioclases. Schweiz. Mineral. Petrog. Mitt. **48**, 53–56 (1968)

Nissen, H.-U.: Exsolution phenomena in bytownite plagioclases. In: The feldspars (W.S. MacKenzie and J. Zussman, eds.), pp. 491–521. Manchester: Manchester University Press 1974

Nord, G.L., Jr., Heuer, A.H., Lally, J.S.: Transmission electron microscopy of substructures in Stillwater bytownites. In: The feldspars (W.S. MacKenzie and J. Zussman, eds.), pp. 522–535. Manchester: Manchester University Press 1974

Nord, G.L., Jr., Lally, J.S., Heuer, A.H., Christie, J.M., Radcliffe, S.V., Griggs, D.T., Fisher, R.M.: Petrologic study of igneous and metaigneous rocks from Apollo 15 and 16 using high voltage transmission electron microscopy. Proc. Lunar Sci. Conf. Fourth. Geochim. Cosmochim. Acta, Suppl. 4, **1**, 953–970 (1973)

Pashley, D.W., Presland, A.E.B.: The observation of antiphase boundaries during the transition from CuAuI to CuAuII. J. Inst. Metals **87**, 419–428 (1959)

Planansky, G.A.: The Bridges Area (S.A. Morse, ed.), The Nain Anorthosite Project, Labrador: Field Report 1972, Contr. 11. Geology Department, University of Massachusetts, Amherst, Massachusetts, pp. 83–89 (1972)

Ribbe, P.H.: The chemistry, structure and nomenclature of feldspars. In: Feldspar mineralogy (P.H. Ribbe, ed.), Vol. 2, pp. R1–R72, Mineral. Soc. Amer. Short Course Notes, 1975

Richey, J.E., Thomas, H.H.: The geology of Ardnamurchan, Northwest Mull and Coll. Memoir Geol. Sur. Scotland. 393 pp. (1930)

Robinson, P.: Gneiss domes of the Orange Area, Massachusetts, and New Hampshire, Ph.D. thesis, Harvard University 253 pp. (1963)

Robinson, P.: Alumino-silicate polymorphs and Paleozoic erosion rates in central Massachusetts (Abs.). Am. Geophys. Union Trans. **47**, 424 (1966)

Robinson, P., Jaffe, H.W.: Aluminous enclaves in gedrite-cordierite gneiss from southwestern New Hampshire. Am. J. Sci. **267**, 389–421 (1969)

Roeder, P.L., Osborn, E.F.: Experimental data for the system MgO-FeO-Fe_2O_3-$CaAl_2Si_2O_8$-SiO_2 and their petrologic implications. Am. J. Sci. **264**, 478–481 (1966)

Schmidt, R.G.: Volcanic rocks of Saipan, Mariana Islands, Ph.D. thesis, Harvard University, 178 pp. (1953)

Smyth, Joseph R.: Intracrystalline cation order in a lunar crustal troctolite. Proc. Lunar Sci. Conf. Sixth. Geochim. Cosmochim. Acta, Suppl. 6, **1**, 821–832 (1976)

Toman, K., Frueh, A.J.: Modulated structure of an intermediate plagioclase: I. Model and computation. Acta Cryst. **B32**, 521–525 (1975a)

Toman, K., Frueh, A.J.: Modulated structure of an intermediate plagioclase: II. Numerical results and discussion. Acta Cryst. **B32**, 526–538 (1975b)

Walker, D., Grove, T.L., Longhi, J., Stolper, E.M., Hays, J.F.: Origin of lunar feldspathic rocks. Earth Planet. Sci. Lett. **20**, 325–336 (1973)

Wenk, E., Wenk, H.-R., Glauser, A., Schwander, H.: Intergrowth of andesine and labradorite in marbles of the Central Alps. Contrib. Mineral. Petrol. **53**, 311–326 (1975)

Wenk, H.-R., Müller, W.F., Thomas, G.: Antiphase domains in lunar plagioclase. Proc. Lunar Sci. Conf. Fourth. Geochim. Cosmochim. Acta, Suppl. 4, **1**, 909–923 (1973)

Wheeler, E.P.: Anorthosite adamellite complex of Nain, Labrador. Geol. Soc. Am. Bull. **71**, 1755–1762 (1960)

Received August 3, 1976 / Accepted May 3, 1977